



# Multifunctional Polymer Nanocomposites for Non-Enzymatic Glucose Detection: A Brief Review

Bo Wu,<sup>1</sup> Qizhou Xue,<sup>2</sup> Yuxin Fan,<sup>2</sup> Dapeng Cui,<sup>1,\*</sup> Yunlong Sun,<sup>1</sup> Ben Bin Xu,<sup>3</sup> Huige Wei,<sup>2,\*</sup> Handong Li,<sup>3</sup> Priyanka Wasnik,<sup>3</sup> Deepak Sridhar,<sup>4</sup> Hassan Algadi,<sup>5</sup> Zhanhu Guo<sup>3,\*</sup> and Sri Hari Kumar Annamareddy<sup>6,\*</sup>

## Abstract

Glucose sensors have been widely used for clinical diagnostics, environmental monitoring, and food industries. Traditional enzymatic glucose sensors are limited for practical applications due to the restriction of enzymes. In this context, non-enzymatic glucose sensors with metal nanoparticles as redox centers have become a prominent area of current research. However, the catalytic activity of metal nanoparticles is limited by their agglomeration and poor conductivity. In recent years, combining metal nanoparticles with highly conductive polymers to prepare multifunctional polymer nanocomposites (MPNCs) has become a popular strategy to overcome these problems. In this paper, the most recent progress in MPNCs for non-enzymatic glucose detection are briefly reviewed, and the challenges and perspectives are also discussed.

**Keywords:** Polymer; Nanocomposites; Multifunctional; Non-enzymatic glucose sensor.

Received: 03 August 2022; Revised: 31 March 2023; Accepted: 01 April 2023.

Article type: Review article.

## 1. Introduction to glucose sensors and MPNCs

### 1.1 Glucose sensors

Diabetes is a serious metabolic disease characterized by hyperglycemia. In today's society, sedentary work and unhealthy eating habits are accelerating the increase in the number of diabetics worldwide. By the end of 2021, 537 million people had diabetes worldwide, an increase of 74

million from 2019.<sup>[1-3]</sup> Especially in the face of COVID-19, diabetics are more vulnerable to infection.<sup>[4-6]</sup> Continuous hyperglycemia and long-term metabolic disorders will lead to the damage of organs or tissues such as heart, brain, microvascular, kidney, eye and nerve, chronic complications such as diabetic cardiovascular disease, diabetic nephropathy, diabetic retinopathy and diabetic neuropathy. They are the main causes of disability and death in diabetic patients. Therefore, it is necessary to monitor and measure blood glucose levels.<sup>[7-10]</sup>

Glucose sensors are widely used in biomedicine and ecological fields to quickly and accurately detect glucose concentration. In general, glucose sensors are classified into two types: enzymatic glucose sensors<sup>[11-13]</sup> and non-enzymatic glucose sensors,<sup>[14,15]</sup> In 1962, Clark and Lyons<sup>[16]</sup> prepared the first enzymatic glucose sensor. In the reaction process, glucose oxidase combined O<sub>2</sub> to oxidize glucose, and the O<sub>2</sub> consumption served as a detection signal. However, the concentration of O<sub>2</sub> was influenced by the surrounding environment.<sup>[17]</sup> Moreover, there are some other problems with enzymatic glucose sensors, including the difficulty of immobilizing glucose oxidase on the electrode and decreased catalytic activity of glucose oxidase affected by pH values, temperature and other environmental factors.<sup>[18,19]</sup> In this context, non-enzymatic glucose sensors have attracted increasing attention for being free from enzymes.<sup>[20,21]</sup> Fig. 1

<sup>1</sup> College of Light Industry Science and Engineering, Tianjin University of Science and Technology, Tianjin, 300457, China.

<sup>2</sup> Tianjin Key Laboratory of Brine Chemical Engineering and Resource Eco-utilization, College of Chemical Engineering and Materials Science, Tianjin University of Science and Technology, Tianjin, 300457, China.

<sup>3</sup> Department of Mechanical and Construction Engineering, Faculty of Engineering and Environment, Northumbria University, Newcastle upon Tyne, NE1 8ST, UK.

<sup>4</sup> Zentek Ltd. 24 Corporate Crt, Guelph, Ontario, N1G 5G5 Canada.

<sup>5</sup> Department of Electrical Engineering, Faculty of Engineering, Najran University, Najran, 11001, Saudi Arabia.

<sup>6</sup> Department of Chemical and Petrochemical Engineering, University of Nizwa, Birkat Al-Mouz 616, Sultanate of Oman.

\*Authors to whom correspondence should be addressed.

E-mail: [dapeng@tust.edu.cn](mailto:dapeng@tust.edu.cn) (D. Cui); [huigewei@tust.edu.cn](mailto:huigewei@tust.edu.cn) (H. Wei); [zhanhu.guo@northumbria.ac.uk](mailto:zhanhu.guo@northumbria.ac.uk) (Z. Guo); [annamareddy@unizwa.edu.om](mailto:annamareddy@unizwa.edu.om) (S. Annamareddy)

shows the detection mechanism of enzymatic glucose sensor (A) and non-enzymatic glucose sensor (B). In recent years, with the development of nanomaterials, researchers have found that functionalized nanomaterials (such as metal-based materials and carbon materials) can serve as active centers for the catalytic oxidation of glucose in non-enzymatic glucose sensors. Among these functional nanomaterials, metal-based materials show better electrocatalytic activity, but they usually suffer from poor electrical conductivity and often aggregate during the preparation process, which gives rise to a decline in the electrocatalytic activity. Fabricating multifunctional polymer nanocomposites (MPNCs) by integrating intrinsically conductive polymers with metal-based materials to enhance the performance has proved to be an effective strategy.

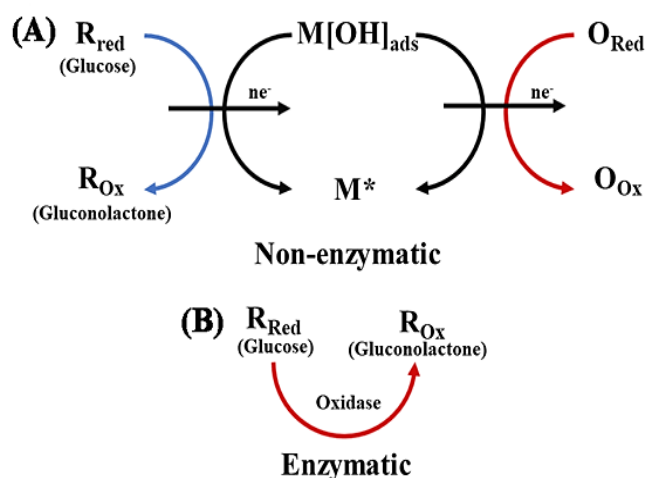


**Fig. 1** Schematic detection mechanism of enzymatic glucose sensor (A) and non-enzymatic glucose sensor (B).

There are many parameters to prove the performance of a glucose sensor. The diffusion effect of glucose is important in electrocatalysis. By testing cyclic voltametric at different scan rates, peak anode current ( $I_{pa}$ ) and peak cathode current ( $I_{pc}$ ) were obtained. Both  $I_{pa}$  and  $I_{pc}$  are linearly correlated with square root of the scanning rate ( $v^{1/2}$ ). The diffusion coefficient ( $D$ ) of electrocatalyzed glucose was calculated using the Randles-Sevcik equation as shown below:<sup>[22]</sup>

$$I_p = 2.69 \times 10^5 n^{3/2} A D^{1/2} C v^{1/2} \quad (1)$$

where  $I_p$  (in A) represents the peak current density,  $n$  represents the electron transfer number (usually 1),  $A$  represents the geometrical area of the electrode surface (in  $cm^2$ ),  $C$  indicates the bulk concentration (in  $mol\ cm^{-3}$ ),  $v$  refers to the scan rate (in  $V\ s^{-1}$ ), and  $D$  represents the diffusion coefficient (in  $cm^2\ s^{-1}$ ). The  $D$  value represents the diffusion of glucose and electrolytes.

The glucose sensor requires a fast response time,<sup>[23]</sup> and in chronoamperometry sensing glucose, the response time of the sensor is judged by the response speed of the current change after adding glucose.

As the most important index of the glucose sensors, sensitivity represents the smallest absolute change that can be detected by the measurement. The higher the sensitivity, the

higher the accuracy of the measurement. Testing the current response of several groups of glucose with different concentrations can obtain a concentration-current response standard curve, that is,  $y=kx+b$ . The slope  $k$  is the sensitivity (in  $A\ mol^{-1}\ cm^{-2}$ ). Limit of detection (LOD) is the lowest concentration of the subject that can be detected in the background signal. The background signal is usually three times the noise with a calculation formula of  $LOD = 3k/S$ , where  $k$  is the slope of the standard curve above and  $S$  is the standard deviation of the detected value of the several blank samples. The sensor performance can be judged by the above parameters.<sup>[24]</sup>

## 1.2 Multifunctional polymer nanocomposites (MPNCs)

MPNCs are defined as “the synthesis of two or more components into a composite material with specific characteristics and properties”.<sup>[25]</sup> According to the matrix, MPNCs are grouped into ceramic composites, carbon composites, metal composites and polymer composites. Since the dimension of at least one component of MPNCs is nano-scale, the performance of MPNCs is better compared to their counterparts of composites with micron-scale.<sup>[26]</sup> Conductive polymers such as polypyrrole (Ppy),<sup>[27]</sup> poly-o-aminophenol (POAP),<sup>[28]</sup> polythiophene (PTh),<sup>[29]</sup> polycarbazole (PTa)<sup>[30]</sup> and polyaniline (PANI)<sup>[31,32]</sup> as depicted in Fig. 2 have been combined with metal-based materials, which exhibit accelerated electron transfer, improved electrocatalytic activity, and enhanced stability compared with only metal-based materials modified electrode.<sup>[33]</sup>

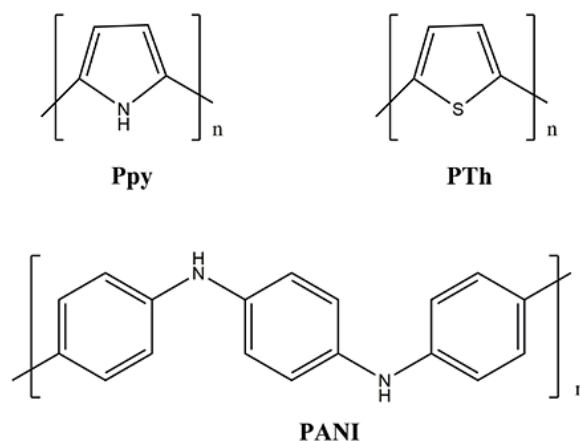


**Fig. 2** The structural formula of Ppy, PTh, and PANI.

This paper is intended to give a brief review of the application of MPNCs combined with metal-based materials, i.e., noble metals, transition metals, and alloy metals, for non-enzymatic glucose sensors. The most recent advances of MPNCs application in non-enzymatic glucose sensor are subsequently presented. Perspectives and challenges of non-enzymatic glucose sensor are also discussed.

## 2. Metal-MPNCs

### 2.1 Noble metal-MPNCs

Platinum (Pt),<sup>[34,35]</sup> gold (Au)<sup>[36-38]</sup> and silver (Ag)<sup>[39]</sup> are used as electrode materials due to the high glucose oxidation currents in alkaline or neutral conditions compared to other metals.<sup>[40,41]</sup>

Unfortunately, the oxidation mechanism of glucose by noble metals is still unclear, although a great amount of research is still being carried out. However, researchers have identified three distinct oxidation regions during the anodic sweep of a Pt-based non-enzymatic glucose sensor. In the potential region of 0.15 -0.3 V vs. RHE (reversible hydrogen electrode), dehydration of organic species such as glucose occurs. This process is considered as the rate-determining step in the oxidation of glucose.<sup>[42]</sup> When the potential region is between 0.4 - 0.8 V vs. RHE, glucose is further oxidized into gluconolactone.<sup>[42]</sup> Meanwhile, Pt is oxidized into PtO when the potential region is positive than 0.8 V vs. RHE.<sup>[43]</sup> However, the region of organic dehydration was not observed in the anodic sweep of the gold-based non-enzymatic glucose sensor.<sup>[44,45]</sup>

Numerous noble metal-MPNCs electrodes have been successfully prepared by various methods, such as template electrodeposition,<sup>[46-48]</sup> hydrothermal,<sup>[49-51]</sup> and selective dissolution.<sup>[52-55]</sup> Xu *et al.*<sup>[56]</sup> synthesized PANI on flexible

carbon cloth (CC) by constant current polymerization. Next, Au nanoparticles (AuNPs) were electrodeposited on the as-prepared PANI/CC electrode by cycle voltammetric (CV) deposition. Fig. 3(A) shows the preparation process of this electrode. The performance of glucose oxidation was tested in 0.5 M NaOH. The CV cycles were changed to control the diameter of AuNPs and the uniformity on the PANI/CC electrode. Results show that AuNPs obtained from 250 cycles of CV were too small to be observed. A large number of AuNPs were uniformly distributed on PANI/CC at 500 CV cycles. The diameter of these AuNPs was about 20 nm. With the number of CV cycles reached 750, the diameter of AuNPs increased to 100 nm and the distribution on PANI/CC was uneven. Excessive CV cycles caused AuNPs to accumulate. As it is well known that the nanomaterials with too large size could decline the catalytic activity.<sup>[57]</sup> And the distribution of AuNPs on PANI/CC electrode was uniform compared with CC electrode. The results of sensitivity test showed that the linear range of AuNPs/CC electrode was similar to that of the

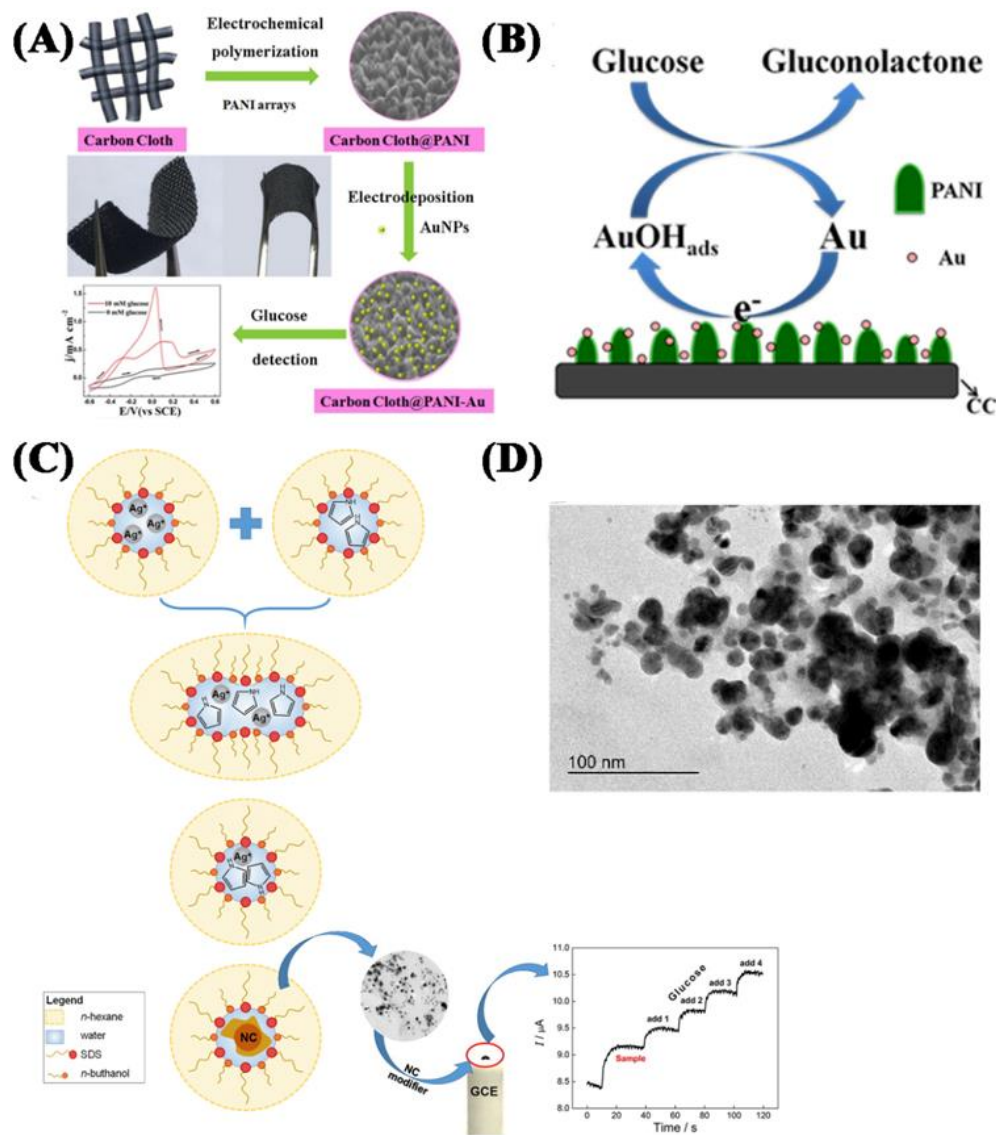


**Fig. 3** (A) Graphical abstract of AuNPs/PANI/CC electrode. (B) Schematic diagram of catalytic mechanism of AuNPs/PANI/CC electrode. Reproduced with permission from [56] Copyright Elsevier (C) Steps on Ppy-AgNPs formation by proposed reverse microemulsion method and detection glucose on GCE. (D) TEM image of Ppy-AgNPs. Reproduced with the permission from [39], Copyright 2017 Elsevier.

AuNPs/PANI/CC electrode, but the sensitivity of former ( $9 \mu\text{A mM}^{-1} \text{cm}^{-2}$ ) was lower than the later ( $150 \mu\text{A mM}^{-1} \text{cm}^{-2}$ ). The electrocatalytic performance was decent as supported by the linear range of  $10.26 \mu\text{M}$ - $10.0 \text{mM}$ , limit of detection (LOD) of  $3.08 \mu\text{M}$  ( $S/N=3$ ). The selectivity towards glucose against various interference molecules of physiological concentrations was excellent, with strong resistance to fructose, D-galactose, ascorbic acid (AA), uric acid (UA), acetaminophen (AMP), NaCl, KCl, *etc.* Fig. 3(B) shows the catalytic mechanism of Au-based non-enzymatic glucose sensor.

Maurício A *et al.* prepared PPy-AgNPs<sup>[39]</sup> nanocomposites by reversed microemulsion approach and evaluated the reaction time to obtain the best nanocomposites for electrocatalytic oxidation of glucose. Fig. 3(C) represents the preparation and sensing process of this sensor. During the preparation process, microemulsion technique was used to promote the formation of a polypyrrole structure with a surfactant of dodecylsulphate as a dopant. Dodecylsulphate as a counter-ion would enhance conjugation and superposition of bipolarions states by immobilizing on the polymeric matrix. Accordingly, it induced a higher molecular order, crystallinity and higher intermolecular conductivity. A series of PPy-AgNPs with different diameters were synthesized by changing the reaction times from 30 to 300 s (30 s, 60 s, 90 s, 120 s, 180 s, 300 s) at the same molar ratio of Ag:Ppy (1:2). Fig. 3(D) shows the TEM images of PPy-AgNPs. Based on tested results, the PPy-AgNPs at shorter reactions times of 30-60 s exhibited smaller diameters and better size distribution and therefore higher sensitivity. With the reaction time longer than 60 s, the increased size of Ag nanoparticles and heterogeneous structure covered by the excess of Ppy would decrease the sensitivity. The PPy-AgNPs (60 s) show the best sensitivity of  $15.1 \mu\text{A L mmol}^{-1}$  at a linear dynamic range (LDR) varying from 25 to  $2500 \mu\text{mol L}^{-1}$  of glucose and limit of detection (signal-to-noise ratio of 3) of  $3.6 \mu\text{mol L}^{-1}$ . Recovery results varied from 99 to 105% for three glucose concentration (30, 50 and  $80 \mu\text{mol L}^{-1}$ ) test in human saliva illustrated that the

accuracy and feasibility of this sensor. Repeatability studies showed that the relative standard deviation (RSD) was only 3.8%.

## 2.2 Transition metal-MPNCs

Noble metals as redox center tend to incur high cost, and their surfaces are prone to poisoning by not only some intermediates produced in the glucose oxidation process, but also the chloride ions present in the tested solution.<sup>[58]</sup> Up to now, plenty of efforts have been made to develop non-enzymatic glucose sensors on the basis of transition metal materials (such as Ni,<sup>[21,59-66]</sup> Co,<sup>[67-69]</sup> and Cu<sup>[70-77]</sup>). The electrocatalytic oxidation of glucose by transition metals mainly involves variable valence states with higher and lower oxidation numbers of the metal.<sup>[78-81]</sup> For example, in a Cu-based non-enzymatic glucose sensor, the reaction centers were  $\text{Cu}^{2+}$  and  $\text{Cu}^{3+}$ . In the reaction process, glucose is oxidized into gluconolactone by  $\text{Cu}^{3+}$ , and finally gluconolactone is hydrolyzed to gluconic acid. Further research shows that the high coincidence of the anodic peak of transition metal and glucose oxidation supports the involvement of the transition metal in this reaction.<sup>[80,81]</sup> However, due to the low conductivity of transition metal oxides, highly conductive substrates are often used to improve the conductivity. MPNCs have been main targets of research motivated not only for higher conductivity, but also for improved uniformity of transition metals on the electrode.<sup>[82]</sup>

Ali *et al.*<sup>[83]</sup> used dialysis tubing membranes to fabricate polyaniline nanofiber (PANI-NFs) on fluorine doped tin oxide (FTO). Fig. 4 exhibits the typical preparation process of this electrode. Compared to the bulk method (i.e. without dialysis tubing membrane), PANI-NFs have been synthesized with much more uniform diameter when monomers were gradually released by the dialysis tubing membrane. Moreover, dimensions of the synthesized nanofibers with bulk method (70-120 nm) are longer compared with the nanofibers with membrane method (50-70 nm). After then, CuO nanoparticles were deposited on PANI-NFs by the electrodeposition method.

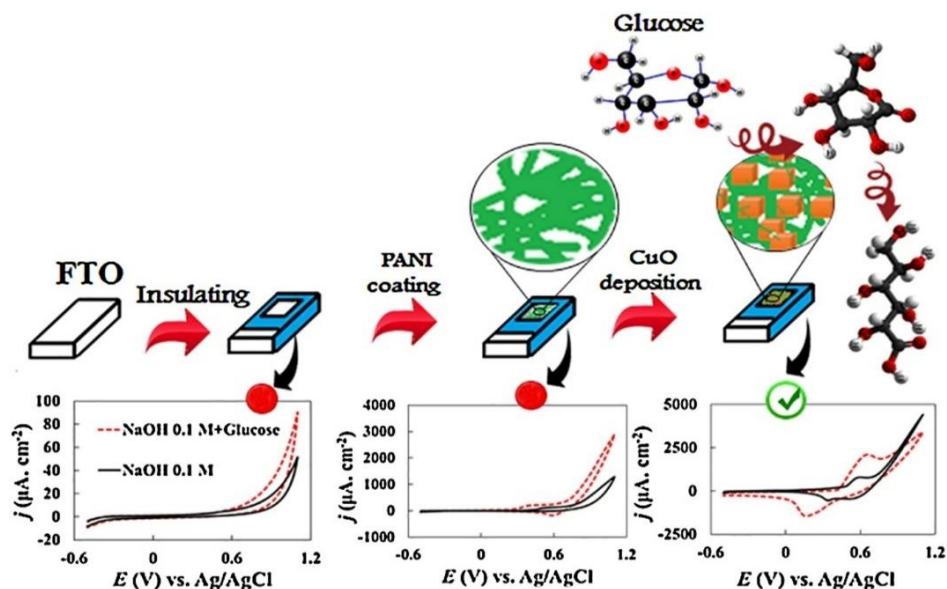


**Fig. 4** The preparation and sensing process of CuO/PANI-NFs/FTO electrode. Reproduced with the permission from [83], Copyright 2018 Elsevier.



The cyclic voltammograms (CVs) of FTO, PANI-NFs/FTO, CuO/FTO and CuO/PANI-NFs/FTO in 0.05 M NaOH solution in the absence and presence of 1 mM glucose showed the significant catalytic effect difference. For the FTO electrode, there was no redox peak in the presence 1 mM glucose and NaOH. PANI-NFs/FTO electrode showed considerable catalytic effect with a small redox peak. The redox peak was observed when CuO/FTO electrode was used, and the catalytic effect and the redox peak current were considerably increased when CuO is deposited on PANI-NFs/FTO electrode. It might be that the PANI/NFs had a larger specific surface area with many microgaps existing between the nanocomposites, and thus CuO could be easily immobilized with high loading and activity. The oxidation peak current on CuO/PANI-NFs/FTO around 0.6 V was about three times higher than those of the CuO/FTO and PANI-NFs/FTO electrodes. This means that the PANI-NFs helped to decorate CuO on the electrode, while the CuO improved the electrocatalytic oxidation of glucose. The amperometric tests verified that the CuO/PANI-NFs/FTO electrode had higher sensitivity to glucose (linear response range: 0.00025 mM-0.28 mM, sensitivity: 2800  $\mu\text{A cm}^{-2} \text{mM}^{-1}$ ; linear response range: 0.28 mM-4.6 mM, sensitivity: 1359  $\mu\text{A cm}^{-2} \text{mM}^{-1}$ , LOD: 0.24  $\mu\text{A}$ ). The repeatability test indicated that the relative standard deviation percentage (RSD%) was 4.9%. The stability of electrode during eleven days was acceptable.

Gamze *et al.*<sup>[84]</sup> synthesized non-enzymatic glucose sensor based on a graphite rod electrode (GRE) modified with biomimetic-composite consisting of Ni nanoparticles (Ni-NPs) and Ppy prepared by electropolymerization of pyrrole monomers. Fig. 5(A) shows the preparation process. SEM images presented that the morphology of GRE was remarkably changed by the electrochemical deposition of Ppy. Ni-NPs formed on the surface of Ni-NPs/Ppy/GRE were much more homogeneous than on Ni-NPs/GRE electrodes. AFM images elucidated that the average thickness of Ppy, Ni-NPs and Ni-NPs/Ppy were 500, 800, and 500 nm, respectively. EIS test results showed that the Ni-NPs/Ppy(1)/GRE had the lowest charge transfer resistance ( $\Delta R_{ct} = \sim 17 \Omega$ ) compared with GRE ( $\sim 380 \Omega$ ), Ppy/GRE ( $\sim 30 \Omega$ ), Ni-NPs/GRE ( $\sim 45 \Omega$ ). In addition, the effects of cycle number during the electrochemical deposition of Ppy layer and the order of electrochemical formation of Ppy layer with electrodeposition of Ni-NPs on the response to glucose were investigated. The Ni-NPs/Ppy<sub>(1)</sub>/GRE and Ni-NPs/Ppy<sub>(2)</sub>/GRE and Ni-NPs/Ppy<sub>(5)</sub>/GRE electrode were prepared by the adjustment of number of potential cycles performed during the electrochemical deposition of Ppy layer (Ppy<sub>(1)</sub>, Ppy<sub>(2)</sub> and Ppy<sub>(5)</sub> represent the numbers of potential cycles, respectively). The recorded CVs in the solution containing 0.10 mol L<sup>-1</sup> of NaOH and 2.0 mmol L<sup>-1</sup> of glucose indicated that the Ni-NPs/Ppy<sub>(1)</sub>/GRE electrode had the optimal catalytic performance. Then another electrode was prepared where the order of Ppy and Ni-NPs was in opposite way (Ppy<sub>(1)</sub>/Ni-NPs/GRE). Results showed that the catalytic effect was weaker than that of Ni-NPs/Ppy<sub>(1)</sub>/GRE. This effect was related to hindered diffusion of glucose through Ppy layer towards electro-catalytic NiO(OH) structures. The result of

the amperometric determination of glucose showed that the sensitivity and LOD were estimated to be 2873  $\mu\text{A mmol}^{-1} \text{L cm}^{-1}$  and 0.4  $\mu\text{mol L}^{-1}$  for Ni-NPs/Ppy<sub>(1)</sub>/GRE and 1387  $\mu\text{A mmol}^{-1} \text{L cm}^{-1}$  and 0.7  $\mu\text{mol L}^{-1}$  for Ni-NPs/GRE, respectively. The stability and anti-interference of the electrode were acceptable. Figs. 5(B) and (C) show the CVs of GRE, Ppy<sub>(1)</sub>/GRE, Ni-NPs/GRE and Ni-NPs/Ppy<sub>(1)</sub>/GRE electrode.

### 2.3 Alloy metal-MPNCs

More and more studies have shown that the heteroatoms inside the alloy metal electrode can influence the activation or the binding energy of the solution, always leading to a new reaction pathway and reduced overpotential.<sup>[32]</sup> Computational chemistry have extensively explained that the metal alloy electrode had higher electrical conductivity, catalytic efficiency, anti-interference and stability compared with the single metal electrode.

Shen *et al.*<sup>[85]</sup> prepared Ppy/GO support by in situ chemical polymerization of pyrrole monomer. NiCo nanoparticles were synthesized on the Ppy/GO surface by hydrothermal method. Combination of the Ppy and NiCo nanoparticles on GO surface synergistically enhanced the catalytic efficiency and improved anti-interference compared with single component systems such as Ppy/GO and NiCo/GO. Kh. Ghanbari *et al.*<sup>[86]</sup> electrodeposited Ni and Cu nanoparticles on PANI substrate. Then, the obtained Cu nanoparticles or Ni nanoparticles modified PANI film electrode was put in 0.05 M NaOH solution, and the potential was scanned in order to allow the Cu/Ni nanoparticles to be oxidized into oxide. SEM, XRD, FT-IR and Roman confirmed that the PANI/GCE, CuO/PANI/GCE, NiO/PANI/GCE and CuO/NiO/PANI/GCE electrode had been successfully prepared. The electrochemical behavior of these electrodes were investigated using CV in 0.1 M NaOH in the potential window ranging from 0.0 to 0.8 V with a scan rate of 50 mV s<sup>-1</sup>. There was no redox peak observed on the PANI/GCE, indicating that PANI could not undergo the redox reaction. However, NiO/PANI/GCE exhibited an oxidation peak at 0.60 V and a reduction peak at 0.37 V, which were assigned to Ni(II)/Ni(III) redox couple forming in alkaline medium. Meanwhile, no redox peaks could be observed at the CuO/PANI/GCE electrode under the same condition. CuO/NiO/PANI/GCE electrode exhibited a pair of well-defined redox peaks with the anodic peak at approximately 0.57 V and the cathodic peak at 0.41 V. This redox peaks should be ascribed to Ni(II)/Ni(III) redox couple. It's worth noting that the oxidation peak current at the CuO/NiO/PANI/GCE electrode was three times higher than that of NiO/PANI/GCE electrode. In fact, the doping of CuO increased the amount of Ni<sup>3+</sup> at the electrode surface during the electrochemical reactions. As we know, the Ni<sup>3+</sup> were considered as lattice defects contributing to enhanced electrical conductivity, but the amount of Ni<sup>3+</sup> was limited by the reaction. But the doping of CuO increased the amount of Ni<sup>3+</sup> at the electrode surface. Therefore, the doping of CuO significantly increased the redox peak current at the NiO/CuO/PANI/GCE electrode compared than NiO/PANI/GCE electrode.

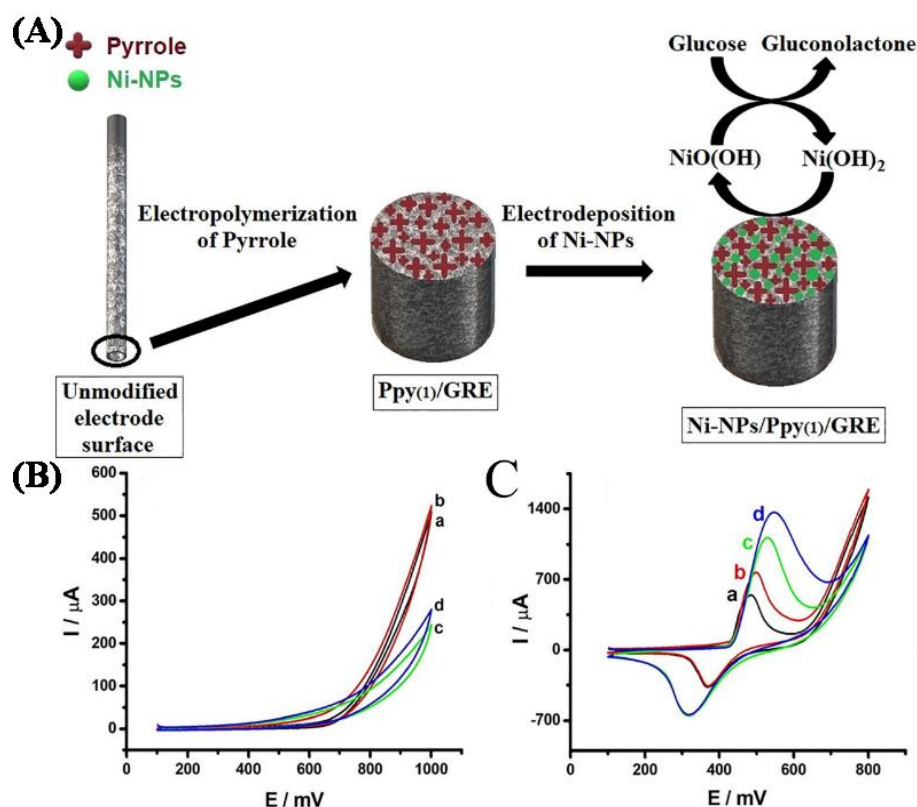


**Fig. 5** (A) The preparation process of Ni-NPs/Ppy/GRE electrode. CVs of: (B) – bare GRE (curves a, b) and Ppy<sub>(1)</sub>/GRE (curves c, d); (C) – Ni-NPs/GRE (curves a, b) and Ni-NPs/Ppy<sub>(1)</sub>/GRE (curves c, d) recorded in the absence (a, c) and presence of 2.0 mmol L<sup>-1</sup> solution of glucose (curves b, d). Reproduced with permission from [84], Copyright 2021 Elsevier

Duan *et al.*<sup>[87]</sup> prepared a NiCo<sub>2</sub>O<sub>4</sub>@Ppy/nickel foam (NF) electrode by combing oxidation polymerization and hydrothermal method (Fig. 6A). This electrode presented a higher catalytic activity to glucose oxidation than monometallic oxide electrode (Co<sub>3</sub>O<sub>4</sub>@Ppy/NF and NiO@Ppy/NF) because of a synergy of the bimetallic oxide. In addition, due to the excellent conductivity of Ppy, the transmitting charges among electrode material were enhanced. Moreover, the Ppy could enhance the stability of NiCo<sub>2</sub>O<sub>4</sub> on the electrode surface and prevented it from leaving the electrode in the reaction. CV results showed that NiCo<sub>2</sub>O<sub>4</sub>@Ppy/NF electrode had higher redox current and lower anodic peak potential by combing NiCo<sub>2</sub>O<sub>4</sub> with Ppy compared with the three other electrodes (NF, NiCo<sub>2</sub>O<sub>4</sub>/NF and Ppy/NF). The NiCo<sub>2</sub>O<sub>4</sub>@Ppy/NF electrode only had a positive shift of 15 mV in a glucose concentration range of 1.0-2.0 mM, but the positive shift was 65 mV in the case of NiCo<sub>2</sub>O<sub>4</sub>/NF electrode under the same condition. EIS results also indicated that the  $R_{et}$  (electron transfer-limited process) of NiCo<sub>2</sub>O<sub>4</sub>@Ppy/NF electrode (9.70 Ω) is significantly lower than that of NiCo<sub>2</sub>O<sub>4</sub>/NF electrode (28.71 Ω). These results suggest that the Ppy played an important role in transmitting charges among the electrode. The polarization curves of NiCo<sub>2</sub>O<sub>4</sub>@Ppy/NF electrode indicated that Ppy could protect the inner catalyst compared with exposed NiCo<sub>2</sub>O<sub>4</sub>/NF electrode. On the other hand, the Co<sub>3</sub>O<sub>4</sub>@Ppy/NF and NiO@Ppy/NF electrode showed that the peak potential shifted to positive under the same condition compared with the NiCo<sub>2</sub>O<sub>4</sub>@Ppy/NF electrode. The results suggested that the

number of catalytic sites and effective ion channels for glucose electro oxidation would increase after the Ni atom entered the crystal lattice of Co<sub>3</sub>O<sub>4</sub>. Amperometric measurements results showed that the sensitivity of NiCo<sub>2</sub>O<sub>4</sub>@Ppy/NF electrode was 3059.25 μA cm<sup>-2</sup> mM<sup>-1</sup> (0.001-0.1 mM), 1919.93 μA cm<sup>-2</sup> mM<sup>-1</sup> (0.1-2 mM), and 659.30 μA cm<sup>-2</sup> mM<sup>-1</sup> (2-20 mM), respectively. The LOD was 0.22 μM (S/N=3). The multi-component synergy of the NiCo<sub>2</sub>O<sub>4</sub>@Ppy/NF electrode not only decreased the distance of electron transportation, but also contributed to constructing an efficient electron route way.

Ali Sedighi *et al.*<sup>[88]</sup> chemically synthesized NiP<sub>0.1</sub>-SnO<sub>x</sub>/PANI/CuO (NTPC) on flexible cotton towards a non-enzymatic glucose sensor (Fig. 6B). The composition of PANI not only helped CuO nanoparticles immobilize on the Ni surface, improved the electrical properties and the amount of CuO nanoparticles, but also enhanced the combination of Ni and Cu oxide. PANI was in-situ synthesized using chemical method on treated fabric to improve the ion transfer on the electrode and help the CuO nanoparticles to be immobilized on the fabric. At last, CuO was synthesized separately and the deposition was carried out through soaking process to prepare the NTPC electrode. SEM images showed that the nickel-activated fabric was coated with nickel-phosphorous particles doped with SnO, SnO<sub>2</sub> and PANI. Unlike the uniform PANI nanoparticles, the NiP-SnO<sub>x</sub> nanoparticles tend to agglomerate due to magnetic forces between nickel particles. It's worth noting that the NiP-SnO<sub>x</sub> nanoparticles were deposited on the nickel nanoparticles on the fabric surface, and therefore avoid the problem above mentioned.

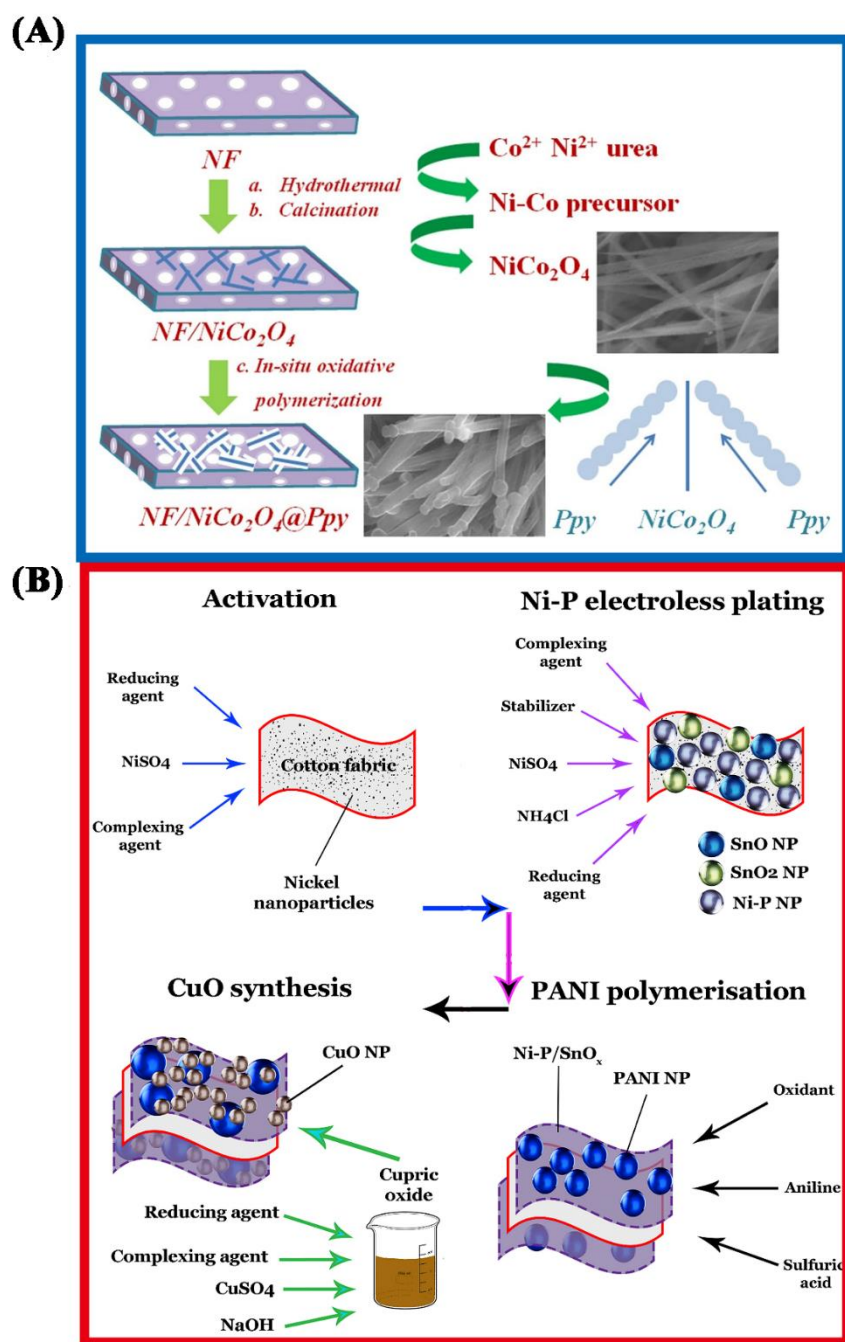


**Fig. 6** The preparation process of  $\text{NiCo}_2\text{O}_4@\text{Ppy}/\text{NF}$  (A) and  $\text{NiP}_{0.1}\text{-SnO}_x/\text{PANI}/\text{CuO}$ . Reproduced with the permission from [87], Copyright 2019 Elsevier (B) electrode. Reproduced with permission from [88], Copyright 2019 Elsevier.

### 3. Summary

In this review, significant progress of metal-MPNCs non-enzymatic glucose sensor has been discussed in the last decade. MPNCs possess unique physicochemical properties with high electrical conductivity, good biocompatibility, environmental stability and low cost, and lead to different interactions, such as charge transfer, electronic interactions and morphological modifications by ssscombined with metal nanoparticles. The noble metal-based sensor has the advantages of operation in neutral pH, but has disadvantages of poor anti-interference, stability and high cost. The transition metal-based sensor can only operate in alkaline conditions due to the redox center (MOH/MOOH), and generally shows superior sensitivity and

wide linear range. The alloy metal-based glucose sensor, due to the bimetallic redox center, exhibits higher electrical conductivity (at least two orders of magnitude) and higher electrocatalytic activity compared with to single metal redox center. The sensitivity, reproducibility and durability are outstanding too.

### 4. Outlook

Metal-MPNCs have drawn huge interest as a redox center to overcome the innate limitations of enzyme sensors, and will be a solution to solve the stability issue and the complicated and irreproducible process for mass production of enzyme sensors. But there are still many problems left, for example, to



operate in whole blood, interferences coming from various electroinactive molecules. In addition, more efforts are needed to look into sensing mechanism and figure out the problems hampering reliable operation for practical use and mass production.

### Acknowledgements

This work is financially supported by Young Elite Scientists Sponsorship Program by Tianjin (TJSQNTJ-2018-03).

### Conflict of Interest

There is no conflict of interest.

### Supporting Information

Not applicable.

### References

- [1] K. Ogurtsova, L. Guariguata, N. C. Barengo, P. L.-D. Ruiz, J. W. Sacre, S. Karuranga, H. Sun, E. J. Boyko, D. J. Magliano, IDF diabetes Atlas: global estimates of undiagnosed diabetes in adults for 2021, *Diabetes Research and Clinical Practice*, 2022, **183**, 109118, doi: 10.1016/j.diabres.2021.109118.
- [2] S. Davies, Y. Hu, J. Blyth, N. Jiang, A. K. Yetisen, Reusable dual-photopolymerized holographic glucose sensors, *Advanced Functional Materials*, 2023, 2214197, doi: 10.1002/adfm.202214197.
- [3] H. Zhu, L. Li, W. Zhou, Z. Shao, X. Chen, Advances in non-enzymatic glucose sensors based on metal oxides, *Journal of Materials Chemistry B*, 2016, **4**, 7333-7349, doi: 10.1039/c6tb02037b.
- [4] Shape the future of diabetes at the IDF World Diabetes Congress 2022, *Diabetes Research and Clinical Practice*, 2022, **187**, 109909, doi: 10.1016/j.diabres.2022.109909.
- [5] Z. Wu, X. Yang, J. Wu, Conductive hydrogel- and organohydrogel-based stretchable sensors, *ACS Applied Materials & Interfaces*, 2021, **13**, 2128-2144, doi: 10.1021/acsami.0c21841.
- [6] M. Wei, Y. Qiao, H. Zhao, J. Liang, T. Li, Y. Luo, S. Lu, X. Shi, W. Lu, X. Sun, Electrochemical non-enzymatic glucose sensors: recent progress and perspectives, *Chemical Communications*, 2020, **56**, 14553-14569, doi: 10.1039/d0cc05650b.
- [7] M. Elanchezian, K. Prakasham, M. Eswaran, M. Duraisamy, S. Ganesan, S. L. Lee, V. Kumar Ponnusamy, Eco-friendly fabrication of nonenzymatic electrochemical sensor based on cobalt/polymelamine/nitrogen-doped graphitic-porous carbon nanohybrid material for glucose monitoring in human blood, *Environmental Research*, 2023, **223**, 115403, doi: 10.1016/j.envres.2023.115403.
- [8] Y. Liu, Q. Yu, L. Ye, L. Yang, Y. Cui, A wearable, minimally-invasive, fully electrochemically-controlled feedback minisystem for diabetes management, *Lab on a Chip*, 2023, **23**, 421-436, doi: 10.1039/d2lc00797e.
- [9] K.-N. Kang, S.-I. Kim, J.-C. Yoon, J. Kim, C. Cahoon, J.-H. Jang, Bi-functional 3D-NiCu-double Hydroxide@Partially etched 3D-NiCu catalysts for non-enzymatic glucose detection and the hydrogen evolution reaction, *ACS Applied Materials & Interfaces*, 2022, **14**, 33013-33023, doi: 10.1021/acsami.2c04471.
- [10] P. GhavamiNejad, A. GhavamiNejad, H. Zheng, K. Dhingra, M. Samarikhalaj, M. Poudineh, A conductive hydrogel microneedle-based assay integrating PEDOT: PSS and Ag-Pt nanoparticles for real-time, enzyme-less, and electrochemical sensing of glucose, *Advanced Healthcare Materials*, 2023, **12**, 2202362, doi: 10.1002/adhm.202202362.
- [11] H. Zhu, L. Li, W. Zhou, Z. Shao, X. Chen, Advances in non-enzymatic glucose sensors based on metal oxides, *Journal of Materials Chemistry B*, 2016, **4**, 7333-7349, doi: 10.1039/c6tb02037b.
- [12] Y. Shu, Y. Yan, J. Chen, Q. Xu, H. Pang, X. Hu, Ni and NiO nanoparticles decorated metal-organic framework nanosheets: facile synthesis and high-performance nonenzymatic glucose detection in human serum, *ACS Applied Materials & Interfaces*, 2017, **9**, 22342-22349, doi: 10.1021/acsami.7b07501.
- [13] Y. Zhang, Y. Liu, L. Su, Z. Zhang, D. Huo, C. Hou, Y. Lei, CuO nanowires based sensitive and selective non-enzymatic glucose detection, *Sensors and Actuators B: Chemical*, 2014, **191**, 86-93, doi: 10.1016/j.snb.2013.08.096.
- [14] Q. Zhang, M. Kaisti, A. Prabhu, Y. Yu, Y.-A. Song, M. H. Rafailovich, A. Rahman, K. Levon, Polyaniline-functionalized ion-sensitive floating-gate FETs for the on-chip monitoring of peroxidase-catalyzed redox reactions, *Electrochimica Acta*, 2018, **261**, 256-264, doi: 10.1016/j.electacta.2017.12.130.
- [15] M. Guler, V. Turkoglu, M. R. Kivanc, A novel enzymatic glucose biosensor and nonenzymatic hydrogen peroxide sensor based on (3-aminopropyl) triethoxysilane functionalized reduced graphene oxide, *Electroanalysis*, 2017, **29**, 2507-2515, doi: 10.1002/elan.201700417.
- [16] L. C. Clark Jr, C. Lyons, Electrode systems for continuous monitoring in cardiovascular surgery, *Annals of the New York Academy of Sciences*, 2006, **102**, 29-45, doi: 10.1111/j.1749-6632.1962.tb13623.x.
- [17] S. Park, Y. J. Song, J.-H. Han, H. Boo, T. Dong Chung, Structural and electrochemical features of 3D nanoporous platinum electrodes, *Electrochimica Acta*, 2010, **55**, 2029-2035, doi: 10.1016/j.electacta.2009.11.026.
- [18] M. Yang, Y. Yang, H. Yang, G. Shen, R. Yu, Layer-by-layer self-assembled multilayer films of carbon nanotubes and platinum nanoparticles with polyelectrolyte for the fabrication of biosensors, *Biomaterials*, 2006, **27**, 246-255, doi: 10.1016/j.biomaterials.2005.05.077.
- [19] M. Yang, Y. Yang, Y. Liu, G. Shen, R. Yu, Platinum nanoparticles-doped Sol-gel/carbon nanotubes composite electrochemical sensors and biosensors, *Biosensors and Bioelectronics*, 2006, **21**, 1125-1131, doi: 10.1016/j.bios.2005.04.009.
- [20] T. Kangkamano, A. Numnuam, W. Limbut, P. Kanatharana, P. Thavarungkul, Chitosan cryogel with embedded gold nanoparticles decorated multiwalled carbon nanotubes modified electrode for highly sensitive flow based non-enzymatic glucose sensor, *Sensors and Actuators B: Chemical*, 2017, **246**, 854-863, doi: 10.1016/j.snb.2017.02.105.



- [21] S. Darvishi, Ni nanoparticle-decorated reduced graphene oxide for non-enzymatic glucose sensing: an experimental and modeling study, *Electrochimica Acta*, 2017, **240**, 388-398, doi: 10.1016/j.electacta.2017.04.086.
- [22] A. Muhs, T. Bobrowski, A. Lielpētere, W. Schuhmann, Catalytic biosensors operating under quasi-equilibrium conditions for mitigating the changes in substrate diffusion, *Angewandte Chemie International Edition*, 2022, **61**, e202211559, doi: 10.1002/anie.202211559.
- [23] Y. Cheng, A touch-actuated glucose sensor fully integrated with microneedle array and reverse iontophoresis for diabetes monitoring, *Biosensors and Bioelectronics*, 2022, **203**, 114026, doi: 10.1016/j.bios.2022.114026.
- [24] S. Cai, C. Xu, D. Jiang, M. Yuan, Q. Zhang, Z. Li, Y. Wang, Air-permeable electrode for highly sensitive and noninvasive glucose monitoring enabled by graphene fiber fabrics, *Nano Energy*, 2022, **93**, 106904, doi: 10.1016/j.nanoen.2021.106904.
- [25] L. George, Handbook of Composites, Van Nostrand Reinhold Co, 1982.
- [26] J. J. Shea, Conducting polymers, fundamentals and applications book review, *IEEE Electrical Insulation Magazine*, 2002, **18**, 60-61, doi: 10.1109/MEI.2002.1015019.
- [27] M. Yan, Y. Yao, J. Wen, L. Long, M. Kong, G. Zhang, X. Liao, G. Yin, Z. Huang, Construction of a hierarchical NiCo<sub>2</sub>S<sub>4</sub>@PPy core-shell heterostructure nanotube array on Ni foam for a high-performance asymmetric supercapacitor, *ACS Applied Materials & Interfaces*, 2016, **8**, 24525-24535, doi: 10.1021/acsami.6b05618.
- [28] R. Ojani, J.-B. Raoof, P. Salmany-Afagh, Electrocatalytic oxidation of some carbohydrates by poly(1-naphthylamine)/nickel modified carbon paste electrode, *Journal of Electroanalytical Chemistry*, 2004, **571**, 1-8, doi: 10.1016/j.jelechem.2004.03.032.
- [29] M. A. Hocevar, G. Fabregat, E. Armelin, C. A. Ferreira, C. Alemán, Nanometric polythiophene films with electrocatalytic activity for non-enzymatic detection of glucose, *European Polymer Journal*, 2016, **79**, 132-139, doi: 10.1016/j.eurpolymj.2016.04.032.
- [30] H. Macit, S. Sen, M. Saçak, Electrochemical synthesis and characterization of polycarbazole, *Journal of Applied Polymer Science*, 2005, **96**, 894-898, doi: 10.1002/app.21532.
- [31] Z. Yu, H. Li, X. Zhang, N. Liu, W. Tan, X. Zhang, L. Zhang, Facile synthesis of NiCo<sub>2</sub>O<sub>4</sub>@Polyaniline core-shell nanocomposite for sensitive determination of glucose, *Biosensors and Bioelectronics*, 2016, **75**, 161-165, doi: 10.1016/j.bios.2015.08.024.
- [32] S. Bilal, W. Ullah, A.-U.-H. Ali Shah, Polyaniline@CuNi nanocomposite: A highly selective, stable and efficient electrode material for binder free non-enzymatic glucose sensor, *Electrochimica Acta*, 2018, **284**, 382-391, doi: 10.1016/j.electacta.2018.07.165.
- [33] D. Zhai, B. Liu, Y. Shi, L. Pan, Y. Wang, W. Li, R. Zhang, G. Yu, Highly sensitive glucose sensor based on Pt nanoparticle/polyaniline hydrogel heterostructures, *ACS Nano*, 2013, **7**, 3540-3546, doi: 10.1021/nm400482d.
- [34] S. Park, T. Dong Chung, H. C. Kim, Nonenzymatic glucose detection using mesoporous platinum, *Analytical Chemistry*, 2003, **75**, 3046-3049, doi: 10.1021/ac0263465.
- [35] Q. Xu, L. Yin, C. Hou, X. Liu, X. Hu, Facile fabrication of nanoporous platinum by alloying-dealloying process and its application in glucose sensing, *Sensors and Actuators B: Chemical*, 2012, **173**, 716-723, doi: 10.1016/j.snb.2012.07.071.
- [36] Y. Z. Su, M. Z. Zhang, X. B. Liu, Z. Y. Li, S. P. Jiang, Development of Au Promoted Pd/C Electrocatalysts for Methanol, Ethanol and Isopropanol Oxidation in Alkaline Medium, *International Journal of Electrochemical Science*, 2012, **7**, 4158-4170.
- [37] X. Z. Li, F. B. Li, Study of Au/Au<sup>3+</sup>-TiO<sub>2</sub> photocatalysts toward visible photooxidation for water and wastewater treatment, *Environmental Science & Technology*, 2001, **35**, 2381-2387, doi: 10.1021/es001752w.
- [38] M.J. Uddin, F. Cesano, D. Scarano, F. Bonino, G. Agostini, G. Spoto, S. Bordiga, A. Zecchina, Cotton textile fibres coated by Au/TiO<sub>2</sub> films: synthesis, characterization and self-cleaning properties, *Journal of Photochemistry and Photobiology A: Chemistry*, 2008, **199**, 64-72, doi: 10.1016/j.jphotochem.2008.05.004.
- [39] M. A. Poletti Papi, F. R. Caetano, M. F. Bergamini, L. H. Marcolino-Junior, Facile synthesis of a silver nanoparticles/polypyrrole nanocomposite for non-enzymatic glucose determination, *Materials Science and Engineering: C*, 2017, **75**, 88-94, doi: 10.1016/j.msec.2017.02.026.
- [40] Y. B. Vassilyev, O. A. Khazova, N. N. Nikolaeva, Kinetics and mechanism of glucose electrooxidation on different electrode-catalysts, *Journal of Electroanalytical Chemistry and Interfacial Electrochemistry*, 1985, **196**, 127-144, doi: 10.1016/0022-0728(85)85085-3.
- [41] S. Biella, L. Prati, M. Rossi, Selective oxidation of D-glucose on gold catalyst, *Journal of Catalysis*, 2002, **206**, 242-247, doi: 10.1006/jcat.2001.3497.
- [42] S. Ernst, J. Heitbaum, C. H. Hamann, The electrooxidation of glucose in phosphate buffer solutions, *Journal of Electroanalytical Chemistry and Interfacial Electrochemistry*, 1979, **100**, 173-183, doi: 10.1016/s0022-0728(79)80159-x.
- [43] E. Skou, The electrochemical oxidation of glucose on platinum—I. The oxidation in 1 M H<sub>2</sub>SO<sub>4</sub>, *Electrochimica Acta*, 1977, **22**, 313-318, doi: 10.1016/0013-4686(77)85079-2.
- [44] M. W. Hsiao, R. R. Adžić, E. B. Yeager, Electrochemical oxidation of glucose on single crystal and polycrystalline gold surfaces in phosphate buffer, *Journal of the Electrochemical Society*, 1996, **143**, 759-767, doi: 10.1149/1.1836536.
- [45] L. A. Larew, D. C. Johnson, Concentration dependence of the mechanism of glucose oxidation at gold electrodes in alkaline media, *Journal of Electroanalytical Chemistry and Interfacial Electrochemistry*, 1989, **262**, 167-182, doi: 10.1016/0022-0728(89)80020-8.
- [46] A. S. Nugraha, C. Li, J. Bo, M. Iqbal, S. M. Alshehri, T. Ahamad, V. Malgras, Y. Yamauchi, T. Asahi, Block-copolymer-assisted electrochemical synthesis of mesoporous gold electrodes: towards a non-enzymatic glucose sensor, *ChemElectroChem*,

- 2017, **4**, 2571-2576, doi: 10.1002/celc.201700548.
- [47] T.-M. Cheng, T.-K. Huang, H.-K. Lin, S.-P. Tung, Y.-L. Chen, C.-Y. Lee, H.-T. Chiu, (110)-exposed gold nanocoral electrode as low onset potential selective glucose sensor, *ACS Applied Materials & Interfaces*, 2010, **2**, 2773-2780, doi: 10.1021/am100432a.
- [48] Y. Li, Y. Y. Song, C. Yang, X. H. Xia, Hydrogen bubble dynamic template synthesis of porous gold for nonenzymatic electrochemical detection of glucose, *Electrochemistry Communications*, 2007, **9**, 981-988, doi: 10.1016/j.elecom.2006.11.035.
- [49] L. Lu, G. Wu, Y. Dong, J. Wang, G. Bai, Green and facile preparation of self-supporting nanoporous gold electrode and effect of ionic liquids on its electrocatalytic oxidation toward glucose, *Journal of Porous Materials*, 2016, **23**, 671-678, doi: 10.1007/s10934-016-0122-2.
- [50] L. Y. Chen, X. Y. Lang, T. Fujita, M. W. Chen, Nanoporous gold for enzyme-free electrochemical glucose sensors, *Scripta Materialia*, 2011, **65**, 17-20, doi: 10.1016/j.scriptamat.2011.03.025.
- [51] Q. Li, S. Cui, X. Yan, Electrocatalytic oxidation of glucose on nanoporous gold membranes, *Journal of Solid-State Electrochemistry*, 2012, **16**, 1099-1104, doi: 10.1007/s10008-011-1501-x.
- [52] Y. A. Chen, Effects of pore size and residual Ag on electrocatalytic properties of nanoporous gold films prepared by pulse electrochemical dealloying, *Electrochimica Acta*, 2015, **153**, 552-558, doi: 10.1016/j.electacta.2014.10.081.
- [53] Y. Xia, W. Huang, J. Zheng, Z. Niu, Z. Li, Nonenzymatic amperometric response of glucose on a nanoporous gold film electrode fabricated by a rapid and simple electrochemical method, *Biosensors and Bioelectronics*, 2011, **26**, 3555-3561, doi: 10.1016/j.bios.2011.01.044.
- [54] Guang-Xian, Zhong, A nonenzymatic amperometric glucose sensor based on three dimensional nanostructure gold electrode, *Sensors and Actuators B: Chemical*, 2015, **212**, 72-77, doi: 10.1016/j.snb.2015.02.003.
- [55] H. Jeong, J. Kim, Electrochemical oxidation of glucose at nanoporous black gold surfaces in the presence of high concentration of chloride ions and application to amperometric detection, *Electrochimica Acta*, 2012, **80**, 383-389, doi: 10.1016/j.electacta.2012.07.040.
- [56] M. Xu, Y. Song, Y. Ye, C. Gong, Y. Shen, L. Wang, L. Wang, A novel flexible electrochemical glucose sensor based on gold nanoparticles/polyaniline arrays/carbon cloth electrode, *Sensors and Actuators B: Chemical*, 2017, **252**, 1187-1193, doi: 10.1016/j.snb.2017.07.147.
- [57] J. Wang, X. Cao, X. Wang, S. Yang, R. Wang, Electrochemical oxidation and determination of glucose in alkaline media based on Au (111)-like nanoparticle array on indium tin oxide electrode, *Electrochimica Acta*, 2014, **138**, 174-186, doi: 10.1016/j.electacta.2014.06.116.
- [58] R. Qiu, X. L. Zhang, R. Qiao, Y. Li, Y. I. Kim, Y. S. Kang, CuNi dendritic material: synthesis, mechanism discussion, and application as glucose sensor, *Chemistry of Materials*, 2007, **19**, 4174-4180, doi: 10.1021/cm070638a.
- [59] H. Nie, Z. Yao, X. Zhou, Z. Yang, S. Huang, Nonenzymatic electrochemical detection of glucose using well-distributed nickel nanoparticles on straight multi-walled carbon nanotubes, *Biosensors and Bioelectronics*, 2011, **30**, 28-34, doi: 10.1016/j.bios.2011.08.022.
- [60] L. Qin, L. He, J. Zhao, B. Zhao, Y. Yin, Y. Yang, Synthesis of Ni/Au multilayer nanowire arrays for ultrasensitive non-enzymatic sensing of glucose, *Sensors and Actuators B: Chemical*, 2017, **240**, 779-784, doi: 10.1016/j.snb.2016.09.041.
- [61] J. Xu, N. Xu, X. Zhang, P. Xu, B. Gao, X. Peng, S. Mooni, Y. Li, J. Fu, K. Huo, Phase separation induced rhizobia-like Ni nanoparticles and TiO<sub>2</sub> nanowires composite arrays for enzyme-free glucose sensor, *Sensors and Actuators B: Chemical*, 2017, **244**, 38-46, doi: 10.1016/j.snb.2016.12.088.
- [62] J. Yang, J.-H. Yu, J. Rudi Strickler, W.-J. Chang, S. Gunasekaran, Nickel nanoparticle-chitosan-reduced graphene oxide-modified screen-printed electrodes for enzyme-free glucose sensing in portable microfluidic devices, *Biosensors and Bioelectronics*, 2013, **47**, 530-538, doi: 10.1016/j.bios.2013.03.051.
- [63] L. Wang, Y. Zhang, J. Yu, J. He, H. Yang, Y. Ye, Y. Song, A green and simple strategy to prepare graphene foam-like three-dimensional porous carbon/Ni nanoparticles for glucose sensing, *Sensors and Actuators B: Chemical*, 2017, **239**, 172-179, doi: 10.1016/j.snb.2016.06.173.
- [64] S. Ci, T. Huang, Z. Wen, S. Cui, S. Mao, D. A. Steeber, J. Chen, Nickel oxide hollow microsphere for non-enzyme glucose detection, *Biosensors and Bioelectronics*, 2014, **54**, 251-257, doi: 10.1016/j.bios.2013.11.006.
- [65] F. J. Garcia-Garcia, P. Salazar, F. Yubero, A. R. González-Elipé, Non-enzymatic Glucose electrochemical sensor made of porous NiO thin films prepared by reactive magnetron sputtering at oblique angles, *Electrochimica Acta*, 2016, **201**, 38-44, doi: 10.1016/j.electacta.2016.03.193.
- [66] M. Li, X. Bo, Z. Mu, Y. Zhang, L. Guo, Electrodeposition of nickel oxide and platinum nanoparticles on electrochemically reduced graphene oxide film as a nonenzymatic glucose sensor, *Sensors and Actuators B: Chemical*, 2014, **192**, 261-268, doi: 10.1016/j.snb.2013.10.140.
- [67] L. Wang, Y. Zhang, Y. Xie, J. Yu, H. Yang, L. Miao, Y. Song, Three-dimensional macroporous carbon/hierarchical Co<sub>3</sub>O<sub>4</sub> nanoclusters for nonenzymatic electrochemical glucose sensor, *Applied Surface Science*, 2017, **402**, 47-52, doi: 10.1016/j.apsusc.2017.01.062.
- [68] C. Zhou, X. Tang, Y. Xia, Z. Li, Electrochemical fabrication of cobalt oxides/nanoporous gold composite electrode and its nonenzymatic glucose sensing performance, *Electroanalysis*, 2016, **28**, 2149-2157, doi: 10.1002/elan.201501177.
- [69] R. Madhu, V. Veeramani, S.-M. Chen, A. Manikandan, A.-Y. Lo, Y.-L. Chueh, Honeycomb-like porous carbon-cobalt oxide nanocomposite for high-performance enzymeless glucose sensor and supercapacitor applications, *ACS Applied Materials & Interfaces*, 2015, **7**, 15812-15820, doi: 10.1021/acsami.5b04132.
- [70] H. Lei, Ultrasensitive and highly selective sandpaper-

- supported copper framework for non-enzymatic glucose sensor, *Electrochimica Acta*, 2017, **248**, 281-291, doi: 10.1016/j.electacta.2017.07.142.
- [71] Libo, Shi, Encapsulating Cu nanoparticles into metal-organic frameworks for nonenzymatic glucose sensing, *Sensors and Actuators B: Chemical*, 2016, **227**, 583-590, doi: 10.1016/j.snb.2015.12.092.
- [72] L. Shi, X. Zhu, T. Liu, H. Zhao, M. Lan, Three-dimensional copper foam supported CuO nanowire arrays: an efficient non-enzymatic glucose sensor, *Electrochimica Acta*, 2017, **235**, 519-526, doi: 10.1016/j.electacta.2017.03.150.
- [73] Xue, Wang, Synthesis of CuO nanostructures and their application for nonenzymatic glucose sensing, *Sensors and Actuators B: Chemical*, 2010, **144**, 220-225, doi: 10.1016/j.snb.2009.09.067.
- [74] W. Xu, S. Dai, X. Wang, X. He, M. Wang, Y. Xi, C. Hu, Nanorod-aggregated flower-like CuO grown on a carbon fiber fabric for a super high sensitive non-enzymatic glucose sensor, *Journal of Materials Chemistry B*, 2015, **3**, 5777-5785, doi: 10.1039/c5tb00592b.
- [75] Y. Zhao, X. Bo, L. Guo, Highly exposed copper oxide supported on three-dimensional porous reduced graphene oxide for non-enzymatic detection of glucose, *Electrochimica Acta*, 2015, **176**, 1272-1279, doi: 10.1016/j.electacta.2015.07.143.
- [76] Y. Zhao, L. Fan, Y. Zhang, H. Zhao, X. Li, Y. Li, L. Wen, Z. Yan, Z. Huo, Hyper-branched Cu@Cu<sub>2</sub>O coaxial nanowires mesh electrode for ultra-sensitive glucose detection, *ACS Applied Materials & Interfaces*, 2015, **7**, 16802-16812, doi: 10.1021/acsami.5b04614.
- [77] C. Dong, H. Zhong, T. Kou, J. Frenzel, G. Eggeler, Z. Zhang, Three-dimensional Cu foam-supported single crystalline mesoporous Cu<sub>2</sub>O nanothorn arrays for ultra-highly sensitive and efficient nonenzymatic detection of glucose, *ACS Applied Materials & Interfaces*, 2015, **7**, 20215-20223, doi: 10.1021/acsami.5b05738.
- [78] S. Berchmans, H. Gomathi, G. P. Rao, Electrooxidation of alcohols and sugars catalysed on a nickel oxide modified glassy carbon electrode, *Journal of Electroanalytical Chemistry*, 1995, **394**, 267-270, doi: 10.1016/0022-0728(95)04099-A.
- [79] M. Juan, Marioli, Electrochemical characterization of carbohydrate oxidation at copper electrodes, *Electrochimica Acta*, 1992, **37**, 1187-1197, doi: 10.1016/0013-4686(92)85055-P.
- [80] K. Kano, M. Torimura, Y. Esaka, M. Goto, T. Ueda, Electrocatalytic oxidation of carbohydrates at copper(II)-modified electrodes and its application to flow-through detection, *Journal of Electroanalytical Chemistry*, 1994, **372**, 137-143, doi: 10.1016/0022-0728(93)03252-K.
- [81] T. R. I. Cataldi, A. Guerrieri, I. G. Casella, E. Desimoni, Study of a cobalt-based surface modified glassy carbon electrode: Electrocatalytic oxidation of sugars and alditols, *Electroanalysis*, 1995, **7**, 305-311, doi: 10.1002/elan.1140070402.
- [82] S. Beg, M. Rahman, A. Jain, S. Saini, P. Midoux, C. Pichon, F. Jalees Ahmad, S. Akhter, Nanoporous metal organic frameworks as hybrid polymer-metal composites for drug delivery and biomedical applications, *Drug Discovery Today*, 2017, **22**, 625-637, doi: 10.1016/j.drudis.2016.10.001.
- [83] A. Esmaeeli, A. Ghaffarnejad, A. Zahedi, O. Vahidi, Copper oxide-polyaniline nanofiber modified fluorine doped tin oxide (FTO) electrode as non-enzymatic glucose sensor, *Sensors and Actuators B: Chemical*, 2018, **266**, 294-301, doi: 10.1016/j.snb.2018.03.132.
- [84] G. Emir, Y. Dilgin, A. Ramanaviciene, A. Ramanavicius, Amperometric nonenzymatic glucose biosensor based on graphite rod electrode modified by Ni-nanoparticle/polypyrrole composite, *Microchemical Journal*, 2021, **161**, 105751, doi: 10.1016/j.microc.2020.105751.
- [85] Q. Sheng, D. Liu, J. Zheng, NiCo alloy nanoparticles anchored on polypyrrole/reduced graphene oxide nanocomposites for nonenzymatic glucose sensing, *New Journal of Chemistry*, 2016, **40**, 6658-6665, doi: 10.1039/c6nj01264g.
- [86] K. Ghanbari, Z. Babaei, Fabrication and characterization of non-enzymatic glucose sensor based on ternary NiO/CuO/polyaniline nanocomposite, *Analytical Biochemistry*, 2016, **498**, 37-46, doi: 10.1016/j.ab.2016.01.006.
- [87] X. Duan, K. Liu, Y. Xu, M. Yuan, T. Gao, J. Wang, Nonenzymatic electrochemical glucose biosensor constructed by NiCo<sub>2</sub>O<sub>4</sub>@Ppy nanowires on nickel foam substrate, *Sensors and Actuators B: Chemical*, 2019, **292**, 121-128, doi: 10.1016/j.snb.2019.04.107.
- [88] A. Sedighi, M. Montazer, S. Mazinani, Synthesis of wearable and flexible NiP0.1-SnOx/PANI/CuO/cotton towards a non-enzymatic glucose sensor, *Biosensors and Bioelectronics*, 2019, **135**, 192-199, doi: 10.1016/j.bios.2019.04.010.

**Publisher's Note:** Engineered Science Publisher remains neutral with regard to jurisdictional claims in published maps and institutional affiliations.